Peertechz

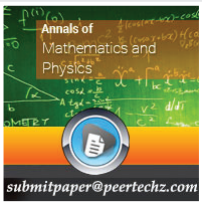

MATHEMATICS AND PHYSICS GROUP

ANNALS OF Mathematics and Physics OPEN ACCESS JOURNAL

ISSN: 2689-7636 DOI: https://dx.doi.org/10.17352/amp

Review Article

Review the Evolution of the Universe

Leonard S Kisslinger*

Department of Physics, Carnegie Mellon University, Pittsburgh PA 15213, USA

Received: 27 March, 2025
Accepted: 16 April, 2025
Published: 17 April, 2025

***Corresponding author:** Leonard S Kisslinger, Department of Physics, Carnegie Mellon University, Pittsburgh PA 15213, USA,
E-mail: kissling@andrew.cmu.edu

Keywords: Evolution; Elementary particles; Basic forces

MSC: 35J25

Abstract

I review elementary particles and basic forces. I review the differential rapidity cross sections for J/Ψ, $\Psi(2S)$, $\Upsilon(1S)$, $\Upsilon(2S)$, $\Upsilon(3S)$, production via p-p, Xe-Xe and O-O collisions, at proton-proton energy $\equiv \sqrt{s_{ppi}} = 5.44$ TeV. I review the production and suppression via Xe-Xe collisions. I review the QCDPT, the Quark Plasma (QGP), the production and potential detection of QGP via Au-Au collisions and magnetic fields produced during the EWPT. In the final section Sterile Neutrinos as Dark Matter is reviewed.

1. Introduction

This review of Xe-Xe collisions is based on the heavy quark state production formalism [1] and the mixed hybrid theory [2]. We also review the suppression scenario [3].

My review is based on the methods used in heavy quark state production in Cu-Cu and Au-Au collisions at $\sqrt{s_{pp}} = 200$ GeV [5] which used the color octet model [6-8]. Prior to the article [3] $\Psi(2S)$ and $\Upsilon(3S)$ suppression in p-Pb collisions was estimated [9] and reviewed [10]. The ALICE collaboration studied J/Ψ production [11]

In section 2, The Evolution of the Universe, including quarks and gluons, is reviewed.

In section 3 and subsection 3.1, I review Elementary Particles, Basic Forces, and. Quantum Chromodynamics.

In section 4 and subsections 4.1, 4.2, and 4.3 Ψ and Υ production via p-p, Xe-Xe, and O-O collisions with $\sqrt{s_{pp}} = 5.44$ TeV are reviewed.

In section 5 and subsection 5.1 Ψ and Υ suppression, mixed hybrid theory, and Ψ suppression in Xe-Xe collisions is reviewed.

In section 6, the QCDPT and the Quark Gluon Condensate are reviewed.

In section 7, the EWPT and the generation of magnetic fields during phase transitions is reviewed.

In section 8, Galaxy Rotation and Dark Matter are reviewed.

In section 9, Sterile Neutrinos as Dark Matter is reviewed.

Section 10 gives Results and Conclusions, ending with the References.

Citation: Kisslinger LS. Review the Evolution of the Universe. Ann Math Phys. 2025;8(2):073-083. Available from: https://dx.doi.org/10.17352/amp.000149

2. The evolution of the universe

The evolution of the Universe is shown in the figure below. The time goes from the Big Bang at 10^{-35} seconds to 14 billion years when we have our present Universe. Recent results are

From Figure 1 at 10^{-35} seconds after the Universe began to inflate due to about 70% of the universe being dark energy, which is anti-gravity. About 27% of the Universe is Dark Matter. Dark Matter particles have no interaction but gravity.

THE EVOLUTION OF THE UNIVERSE
(OVERVIEW)

t = Time	T = Temperature Events
10^{-35} s	10^{14} GeV Big Bang, Strings, Inflation Very early. Current particle theory no good
10^{-11} s	100 GeV Electroweak Phase Transition Particles (Higgs) get masses. Particly theory ok. Baryogenesis? (more particles than antiparticles)
10^{-5} s	100 MeV QCD (quark–hadron) phase transition Quarks(elementary) condense to Protons
1–100 s	Nucleosynthesis: Helium, light nuclei formed 1.0X 10^{9} °K Superconducting Universe
380,000 years	0.25 ev, 3,000 °K Atoms (electrically) neutral Last scattering of light (electromagnetic radiation) from big bang: Cosmic Microwave Background
1 billion years	early galaxies form
14 billion years	2.7 ° K Now

Figure 1: Evolution of the Universe.

Note that at 10^{-11} during the EWPT, magnetic fields were created, and during the Quantum Chromodynamics Phase Transition (QCDPT) at 10^{-5} Quarks were bound by gluons to create protons and neutrons.

3. Elementary particles and basic forces

Elementary particles: Fermions and Bosons. Fermions have Quantum spin =1/2

The elementary Fermions are leptons and quarks. There are three generations of leptons: electron, muon, and tau, with electric charge -1, and their neutrinos with no electric charge. There are three generations of quarks (u,d), (c,s), (t,b).

There are also three anti-leptons. The electron e^- has electric charge -1 while the anti-electron, e^+, has an electric charge +1.

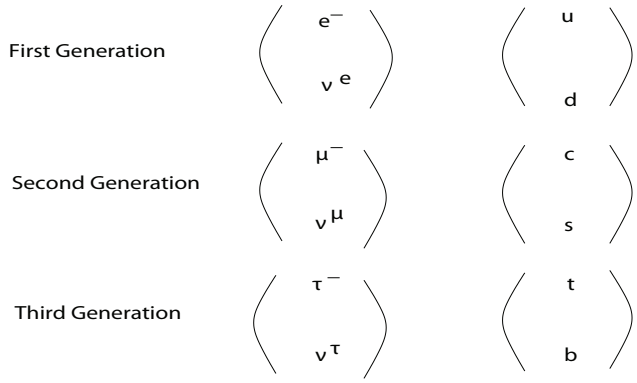

The elementary bosons include the gluon and photon with quantum spin 1.

The production of a photon via coupling to e^-+ e^+ is shown below in Figures 1,2.

4. Quantum Chromodynamics (QCD): Strong interaction field theory

Strong interactions are produced by quarks exchanging gluons, as illustrated in the figure below.

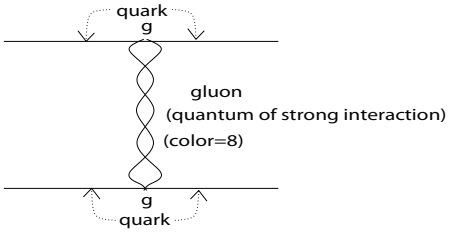

QCD (Quantum Chromodynamics): quark force via gluon exchange
STRONG FORCE

A quark and an antiquark can form a gluon, which has color 8,

$$g^2 \simeq 100 g_e^2 , \quad (1)$$

`` where g is the quark-gluon coupling constant and g_e is the

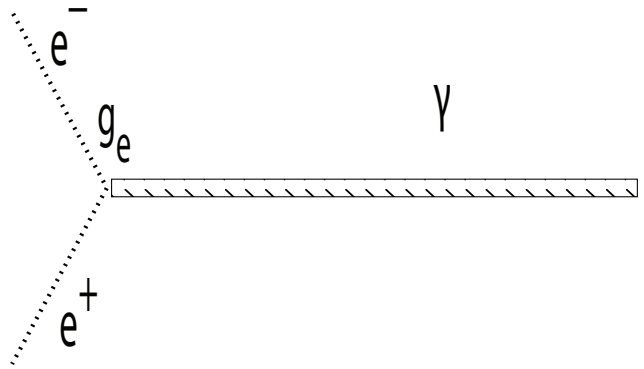

Figure 2: Photon production from e− + e+ collisions with ge the electromagnetic coupling constant.

Citation: Kisslinger LS. Review the Evolution of the Universe. Ann Math Phys. 2025;8(2):073-083. Available from: https://dx.doi.org/10.17352/amp.000149

electromagnetic charge [12]. For $\sqrt{s_{pp}} = 5.44$ TeV the gluon distribution function f_g [13,14] is

$$f_g(\overline{x}(y), 2m) = 1334.21 - 67056.5\overline{x}(y) + 887962.0(\overline{x}(y))^2 . \quad (2)$$

Quarks, which are basic constituents of Quantum Chromo-Dynamics (QCD), interact via the exchange of gluons. QCD is a well-established theory of strong interactions.

4.1. Quark-Gluon Plasma (QGP)

A form of matter, which is called the Quark-Gluon Plasma (QGP), is a thermalized system where the properties of the system are ruled by the quarks and gluons' degrees of freedom. QGP is the QCD analogue of the plasma state of ordinary atomic matter, but the deconfined state, where the deconfined quanta of QGP cannot be observed directly due to the confining property of the QCD vacuum. The only scope to probe such high and dense nuclear matter like QGP, in our laboratories, is possible via relativistic heavy ion collisions.

The QGP is reviewed in section: The QCDPT and the Quark Plasma (QGP).

4.2 Mixed heavy quark hybrid states

The starting point of the method of QCD sum rules [15] is the correlator

$$\Pi^A(x) = \langle | T[J_A(x)J_A(0)] | \rangle , \quad (3)$$

With $|\rangle$ the vacuum state and the current $J_A(x)$ creates the states with quantum numbers A.

With c, $\overline{c}$ and g a charm quark, an anti-charm quark, and a gluon, for the charmonium states, J_c is

$$J_c = fJ_{c\overline{c}} + \sqrt{1-f^2}J_{c\overline{c}g} , \quad (4)$$

where $J_{c\overline{c}}$ creates a normal charmonium state and $J_{c\overline{c}g}$ creates a hybrid state with an active gluon.

The charm quark C needed, with mass [12] $m_c \simeq 1.27$ GeV.

Using QCD sum rules, it was shown that $f \simeq -\sqrt{2}$ for the $\Psi(2S)$ and $\Upsilon(3S)$ heavy quark meson states and $f \simeq 1.0$ for the other charmonium and bottomonium states [2]. vspace4mm

Therefore,

$$| J/\Psi(1S) > \simeq | c\overline{c}(1S) >$$

$$| \Psi(2S) > \simeq -\sqrt{2} | c\overline{c}(1S) > +\sqrt{2} | c\overline{c}g(2S) > , \quad (5)$$

with the $\Psi(2S)$ being a mixed hybrid meson.

Similarly, it was shown with b and $\overline{b}$ a bottom and anti-bottom quark, with mass [12] $m_b \simeq 4.18$ GeV, that $\Upsilon(3S)$ It is also a mixed hybrid meson with

$$| \Upsilon(3S) > \simeq -\sqrt{2} | b\overline{b}(3S) > +\sqrt{2} | b\overline{b}g(3S) > . \quad (6)$$

We need these results for Ψ and production via p-p, Xe-Xe, and O-O collisions are reviewed in the next three subsections.

5. Ψ and ϒ production via p-p, Xe-Xe, and O-O collisions with $\sqrt{s_{pp}} = 5.44$ TeV

The differential rapidity cross section for the production of a heavy quark state Φ with helicity λ = 0 (for unpolarized collisions [14]) In the color octet model via Xe-Xe collisions is given by [5]

$$\frac{d\sigma_{AA\to\Phi(\lambda=0)}}{dy} = R^E_{AA} N^{AA}_{bin} < \frac{d\sigma_{pp\to\Phi(\lambda=0)}}{dy} > , \quad (7)$$

where R^E_{AA} is the product of the nuclear modification factor R_{AA} and S_Φ, the dissociation factor after the state Φ is formed (Figure 3 in Ref [16]). R_{AA} is defined in Ref [17] as

$$R_{AA}(p) = \frac{d^2N^{AA}_{bin}/dpd\eta}{T_{AA}d^2\sigma^{NN}/dpd\eta} . \quad (8)$$

For Xe-Xe collisions we use $R^E_{XeXe} = 0.5$ as $R^E_{AA} \simeq 0.5$ both for Cu-Cu [16,18] and Au-Au [19-21] and $R^E_{PbPb} = 0.5$ was used in Ref [1].

For p-p collisions we use $R^E_{pp} = 0.005$ For O-O collisions we use $R^E_{OO} = 0.25$

5.1. Ψ and ϒ production via p-p collisions with $\sqrt{s_{pp}} = 5.44$ TeV

The differential rapidity cross section for pp collisions

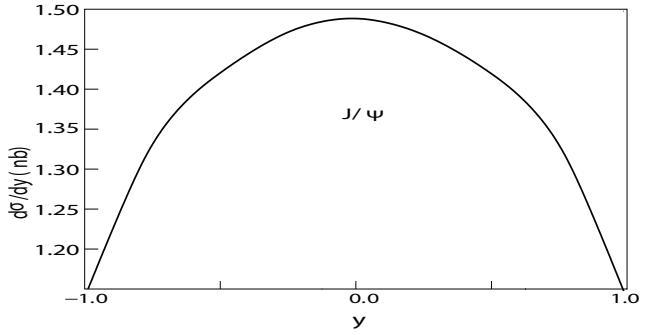

Figure 3: dσ/dy for $2m_c$=3 GeV, $\sqrt{s_{pp}} = 5.44$ TeV via p-p collisions producing J/Ψ with λ = 0.

Citation: Kisslinger LS. Review the Evolution of the Universe. Ann Math Phys. 2025;8(2):073-083. Available from: https://dx.doi.org/10.17352/amp.000149

in terms of f_g [14], the gluon distribution function is

$$\frac{d\sigma_{pp\to\Phi(\lambda=0)}}{dy} = A_\Phi \frac{1}{x(y)} f_g(\overline{x}(y),2m) f_g(a/\overline{x}(y),2m)\frac{dx}{dy}, \quad (9)$$

where from Ref [14] A_Φ = 1.26×10^{-6} nb for Φ = *J*/ and 3.4×10^{-8} nb for Φ = ϒ(1*S*); and $a = 4m^2/s$ = 3.6×10^{-7} for charmonium and 4.0×10^{-6} for bottomonium.

The function $\overline{x}$, the effective parton x in a nucleus (A), is given in Refs [22,23]:

$$x(y) = 0.5[\frac{m}{\sqrt{s_{pp}}}(\exp y - \exp(-y)) + \sqrt{(\frac{m}{\sqrt{s_{pp}}}(\exp y - \exp(-y)))^2 + 4a}]$$

$$\overline{x}(y) = (1+\frac{\xi_g^2(A^{1/3}-1)}{Q^2})x(y). \quad (10)$$

With Ψ(2*S*), ϒ(3*S*) enhanced by $\Pi^2/4$ [14] the differential rapidity cross sections are shown in the following figures. The absolute magnitudes are uncertain, and the shapes and relative magnitudes are our main predictions. In Eq $m = m_c$ = 1.5 GeV for charmonium and $m = m_b$ = 5 GeV for bottomonium quarks.

The differential rapidity cross sections for the production Ψ(1*S*) and Ψ(2*S*) via p-p collisions are shown in the Figures 4-6 below.

5.2. The differential rapidity cross section for the production of a heavy quark state via Xe-Xe collisions

The differential rapidity cross section for the production of a heavy quark state **Φ** with helicity λ = 0 (for unpolarized collisions [14]) in the color octet model via Xe-Xe collisions is given by [5]

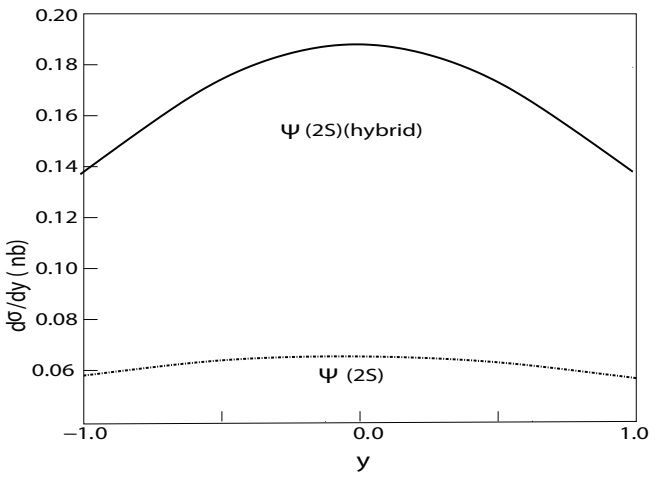

Figure 4: dσ/dy for $2m_c$=3 GeV, $\sqrt{s_{pp}}$ = 5.44 TeV via p-p collisions producing Ψ(2*S*), hybrid theory, with λ = 0 The dashed curve is for the standard $c\overline{c}$ model.

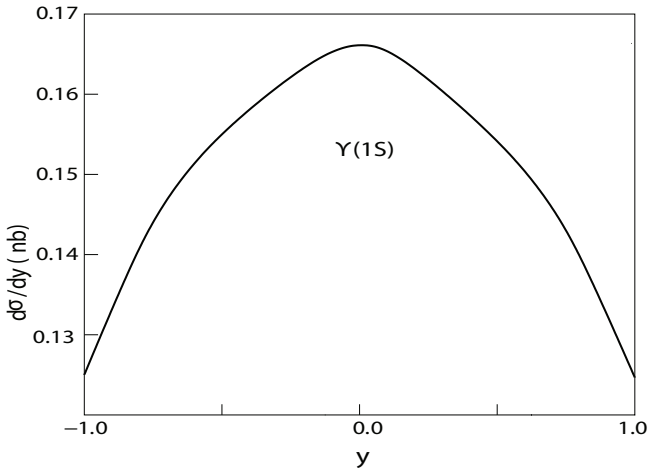

Figure 5: dσ/dy for $2m_b$=10 GeV, $\sqrt{s_{pp}}$ = 5.44 TeV via p-p collisions producing ϒ(1*S*), λ = 0.

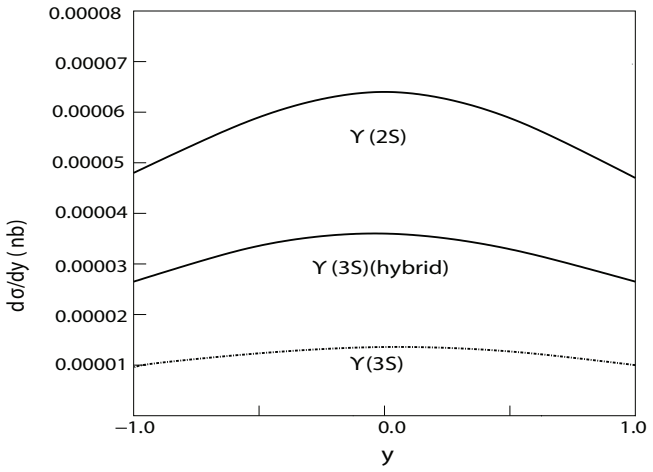

Figure 6: dσ/dy for $2m_b$=10 GeV, $\sqrt{s_{pp}}$ = 5.44 TeV via p-p collisions producing with λ = 0 ϒ(2*S*), and ϒ(3*S*), (hybrid). For ϒ(3*S*), the dashed curve is for the standard $b\overline{b}$ model.

$$\frac{d\sigma_{AA\to\Phi(\lambda=0)}}{dy} = R_{AA}^E N_{bin}^{AA} < \frac{d\sigma_{pp\to\Phi(\lambda=0)}}{dy} >, \quad (11)$$

where R_{AA}^E is the product of the nuclear modification factor R_{AA} and S_Φ, the dissociation factor after the state Φ is formed (see Figure 3 in Ref [16]). R_{AA} is defined in Ref [17] as

$$R_{AA}(p) = \frac{d^2N_{bin}^{AA}/dpd\eta}{T_{AA}d^2\sigma^{NN}/dpd\eta}, \quad (12)$$

where N_{bin}^{AA} is the number of binary collisions in the AA collision, and η is the pseudo-rapidity [24].

Note that $T_{AA} = N_{bin}^{AA}/\sigma^{NN}$, where σ^{NN} is the cross

Citation: Kisslinger LS. Review the Evolution of the Universe. Ann Math Phys. 2025;8(2):073-083. Available from: https://dx.doi.org/10.17352/amp.000149

section for N-N collisions and $< \frac{d\sigma_{pp\to\Phi(\lambda=0)}}{dy} >$ is the differential rapidity cross section for Φ production via nucleon-nucleon collisions in the nuclear medium.

For Xe-Xe collisions we use $R^E_{XeXe} = 0.5$ as $R^E_{AA} \simeq 0.5$ both for Cu-Cu [16,18] and Au-Au [19-21] and $R^E_{PbPb} = 0.5$ was used in Ref [1].

N^{XeXe}_{bin} is the number of binary collisions in Xe-Xe collisions, and $< \frac{d\sigma_{pp\to\Phi(\lambda=0)}}{dy} >$ is the differential rapidity cross section for Φ production via nucleon-nucleon collisions in the nuclear medium.

The number of binary collisions for Pb-Pb from Ref [25] used in Ref [1] was $N^{PbPb}_{bin} \simeq 260.$ The cross sections at $\sqrt{s_{pp}} \simeq 5.0$ TeV [26] $\sigma(b) \simeq 7.66,\ 3.34,\ 5.61$ for PbPb, CuCu, XeXe.

Using $N^{PbPb}_{bin} = 260$, for Cu-Cu collisions $N^{CuCu}_{bin} \simeq 51.5$ [5,25]. From $N^{PbPb}_{bin} = 260$ and the Xe-Xe, Pb-Pb cross sections we estimate $N^{XeXe}_{bin} \simeq 216.$

Therefore in Eq(11) $R^E_{AA} N^{AA}_{bin} \to R^E_{XeXe} N^{XeXe}_{bin} \simeq 108$ with [27] $\xi^2_g = .12 GeV^2$ and Q^2 defined in Ref [22]. Therefore for Xe with $A \simeq 132,\ Q^2 \simeq 10.18\, GeV^2$

$$\bar{x}(y) = 1.048 x(x). \qquad (13)$$

With Ψ(2*S*), Υ(3*S*) enhanced by $\Pi^2/4$ [15] the differential rapidity cross sections are shown in the following figures. The absolute magnitudes are uncertain, and the shapes and relative magnitudes are our main predictions. In Eq(13) $m = m_c = 1.5$ Gev for charmonium and $m = m_b = 5$ Gev for bottomonium quarks (Figures 7-10).

Note that the differential rapidity cross section for the Υ(3*S*) (hybrid) is larger than the differential rapidity cross section for the Υ(3*S*).

5.3. The differential rapidity cross section for the production of a heavy quark state Φ via O-O collisions

This review of heavy quark state production was motivated in part by the article:

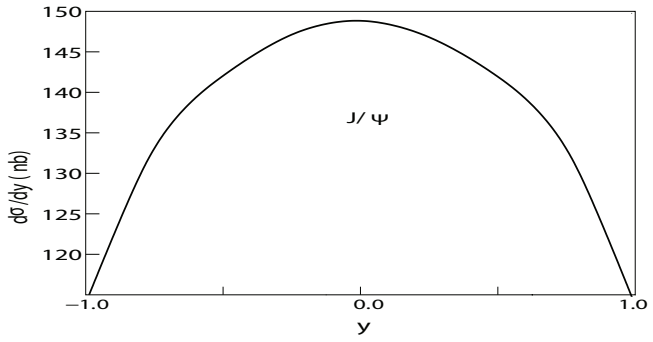

Figure 7: dσ/dy for $2m_c$=3 GeV, $\sqrt{S_{pp}} = 5.44$ TeV via Xe- Xe collisions producing J/Ψ with λ = 0.

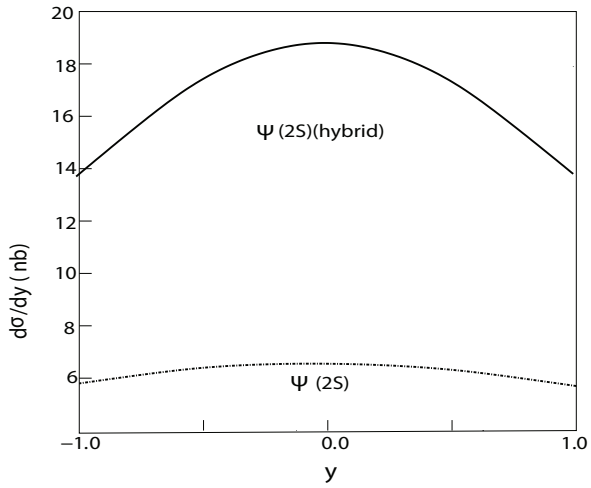

Figure 8: dσ/dy for $2m_c$=3 GeV, $\sqrt{S_{pp}} = 5.44$ TeV via Xe- Xe collisions producing Ψ(2*S*), hybrid theory, with λ = 0.
The dashed curve is for the standard $c\bar{c}$ model.

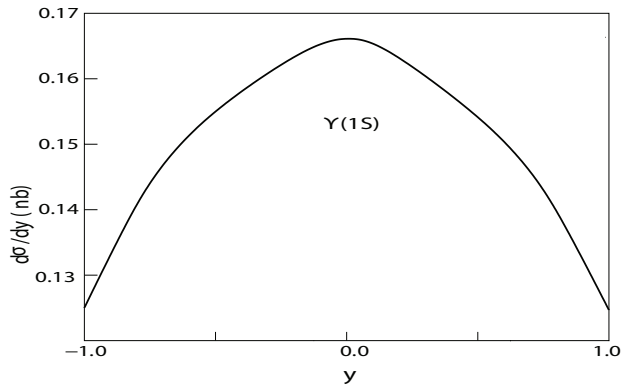

Figure 9: dσ/dy for $2m_b$=10 GeV, $\sqrt{S_{pp}} = 5.44$ TeV via Xe- Xe collisions producing Υ(1*S*), λ = 0.

Opportunities of O-O Collisions at the LHC [28].

For O-O collisions we use $R^E_{OO} = 0.25 = R^E_{XeXe} / 2$.

The differential rapidity cross sections are shown in the following Figures 11-14.

Note that the differential rapidity cross section for the Υ(3*S*) (hybrid) is larger than the differential rapidity cross section for the Υ(3*S*).

Citation: Kisslinger LS. Review the Evolution of the Universe. Ann Math Phys. 2025;8(2):073-083. Available from: https://dx.doi.org/10.17352/amp.000149

6 Ψ and ϒ suppression in Xe-Xe collisions and mixed hybrid theory

The suppression, S_A, of charmonium or bottomonium states is given by the interaction of the meson with nucleons as it traverses the nucleus. From Ref [29]

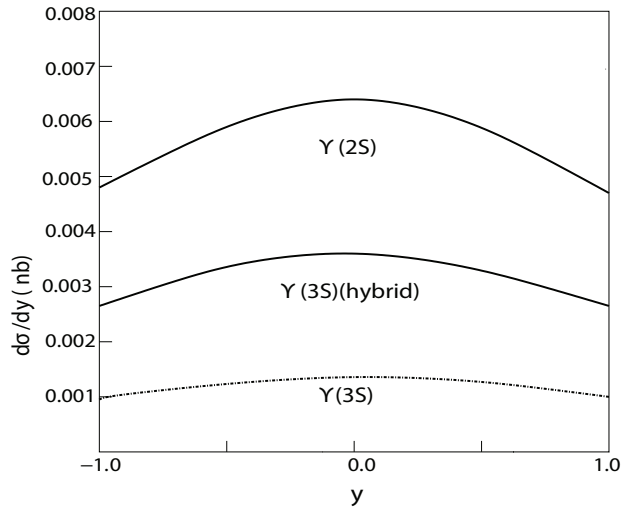

Figure 10: dσ/dy for $2m_b$=10 GeV, $\sqrt{S_{pp}} = 5.44$ TeV via Xe- Xe collisions producing with λ = 0 Υ(2*S*), and Υ(3*S*), (hybrid). For Υ(3*S*), the dashed curve is for the standard $b\bar{b}$ model.

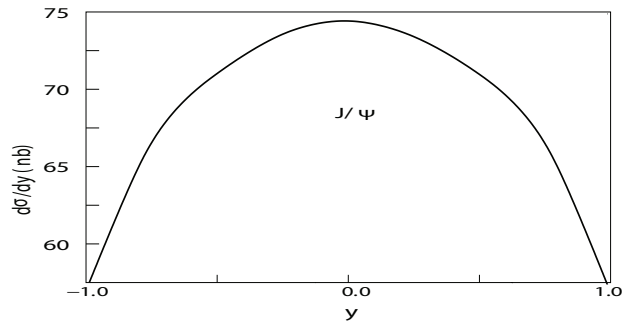

Figure 11: dσ/dy for $2m_c$=3 GeV, $\sqrt{S_{pp}} = 5.44$ TeV via O- O collisions producing J/Ψ with λ = 0

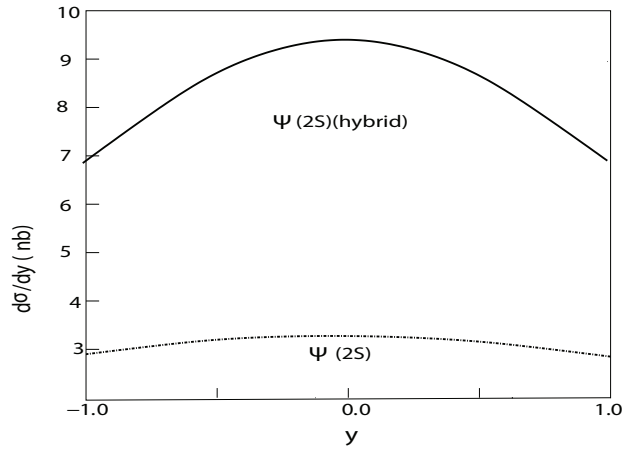

Figure 12: dσ/dy for $2m_c$=3 GeV, $\sqrt{S_{pp}} = 5.44$ TeV via O- O collisions producing Ψ(2*S*), hybrid theory, with λ = 0. The dashed curve is for the standard $c\bar{c}$ model.

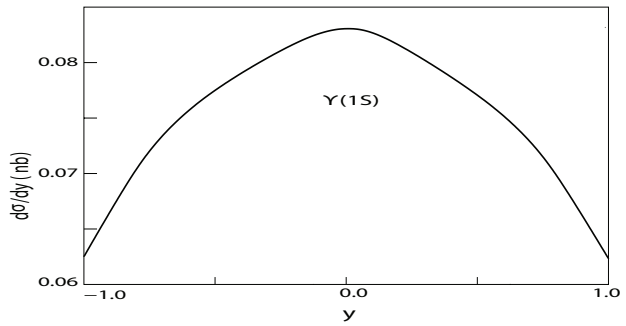

Figure 13: dσ/dy for $2m_b$=10 GeV, $\sqrt{S_{pp}} = 5.44$ TeV via O- O collisions producing Υ(1*S*), λ = 0.

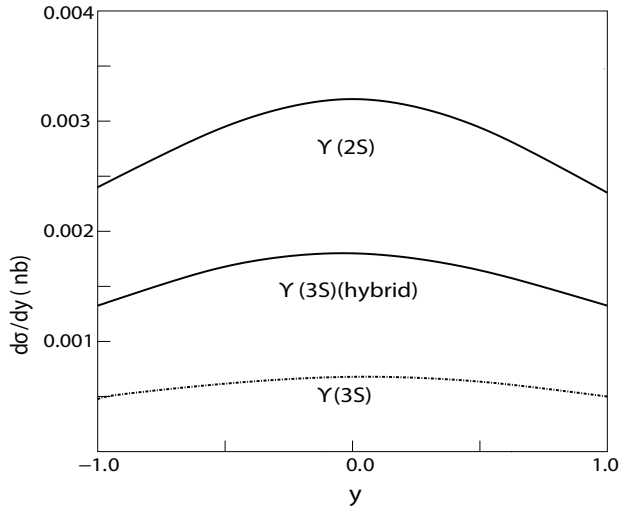

Figure 14: dσ/dy for $2m_b$=10 GeV, $\sqrt{S_{pp}} = 5.44$ TeV via O- O collisions producing with λ = 0 Υ(2*S*), and Υ(3*S*), (hybrid). For Υ(3*S*), the dashed curve is for the standard $b\bar{b}$ model.

$$S_A = e^{-n_o \sigma_{\Phi N} L}, \tag{14}$$

where Φ is a standard $c\bar{c}$, hybrid $c\bar{c}g$ charmonium meson, or a standard $b\bar{b}$, $b\bar{b}g$ bottomonium meson. L is the length the path of Φ in nuclear matter, n_0 = 0.17 fm^{-3} is the nuclear matter density, and $\sigma_{\Phi N}$ is the Φ - N cross section. For Xe-Xe collisions $L \approx 12$ fm.

S_A was estimated for Pb-Pb collisions [1] and p-Pb collisions [9]. From Ref [9] $\sigma_{\Phi N}$ for $\Phi = c\bar{c}, c\bar{c}g, b\bar{b}, b\bar{b}g$ were estimated to be (with a mb → fm^2 correction)

$$\begin{aligned} \sigma_{c\bar{c}N} &\simeq 3.2 \times 10^{-2} \text{ fm}^2 \\ \sigma_{c\bar{c}gN} &\simeq 6.5^2 \text{ fm}^2 \\ \sigma_{b\bar{b}N} &\simeq 2.9 \times 10^{-3} \text{ fm}^2 \\ \sigma_{b\bar{b}gN} &\simeq 0.59 \text{ fm}^2 . \end{aligned} \tag{15}$$

Note that the present results for $n_o \sigma_{\Phi N} L$ differ from

Citation: Kisslinger LS. Review the Evolution of the Universe. Ann Math Phys. 2025;8(2):073-083. Available from: https://dx.doi.org/10.17352/amp.000149

those in Ref [9] for Pb-Pb suppression by a factor of about 1.25 as $L \simeq 15$ fm for Pb and 12 fm for Xe.

6.1 Ψ suppression in Xe-Xe collisions

From Eq. for $J/\Psi = \Psi(1S) = |c\bar{c};1S>$

$$n_o \sigma_{c\bar{c}N} L \simeq 0.065$$
$$S_A^{c\bar{c}} = e^{-n_o \sigma_{c\bar{c}N} L} \simeq 1.0\,, \tag{16}$$

thus the $J/\Psi = \Psi(1S)$ meson appears unsuppressed in Xe-Xe collisions. For a charmonium hybrid meson $c\bar{c}g$ with L=12 fm

$$n_o \sigma_{c\bar{c}gN} L \simeq 13.3$$
$$S_A^{c\bar{c}g} \simeq e^{-13.3} \simeq 0.0\,. \tag{17}$$

Since from Eq(1) the Ψ(2*S*) is 50% standard and 50% hybrid

$$S_A^{\Psi(2S)} \simeq (1+0.0)/2 \simeq 0.5\,. \tag{18}$$

Using the definition of $R^{\Psi(2S)-J/\Psi(1S)}$ of the suppression ratio, the ratio between Ψ(2*S*) to the Ψ(1*S*) states, from Eqs.

$$R^{\Psi(2S)-J/\Psi(1S)}|_{Xe-Xe-theory} \simeq 0.5\,, \tag{19}$$

The experimental result [30] for d-Au collisions and [31] for p-Pb collisions is

$$R^{\Psi(2S)-J/\Psi(1S)}|_{exp} \simeq 0.65 \pm 0.1 \tag{20}$$

which is somewhat larger than $R^{\Psi(2S)-J/\Psi(1S)}|_{Xe-Xe-theory}$.

6.2 ϒ suppression in Xe-Xe collisions

From Eq. for $\Upsilon(1s) = |b\bar{b};1S>$

$$n_o \sigma_{b\bar{b}N} L \simeq 0.0$$
$$S_A^{b\bar{b}} \simeq 1.0.\,, \tag{21}$$

Thus the ϒ(1*S*) and ϒ(2*S*) mesons are not suppressed.

For a hybrid bottomonium meson $b\bar{b}g$ from Eq.

$$n_o \sigma_{\bar{b}gNL} \simeq 1.2$$
$$S_A^{b\bar{g}} \simeq 0.3\,. \tag{22}$$

For the mixed hybrid ϒ(3*S*)

$$S_A^{\Upsilon(3S)} \simeq (1+.3)/2 \simeq 0.65\,. \tag{23}$$

Therefore for Xe-Xe collisions the ϒ(3*S*) suppression is moderate and could be measured in future CERN LHC experiments.

7. The QCDPT and the Quark Plasma (QGP)

The QCDPT is the transition from a universe with dense matter called the quark gluon plasma (QGP), to our universe with protons and neutrons and other hadrons.

As the figure below illustrates, for Au-Au collisions the emission of mixed hybrid mesons, the Ψ(2*S*) and ϒ(3*S*) as discussed above, with active gluons, could be a signal of the formation of the QGP (Figure 15).

The study of the QGP requires reference measurements from systems in which the QGP is not expected to be formed, such as p+p and p+A collisions. The transverse size of the overlap region is comparable to that of a single proton, in systems like p+p and p+A and hence the formation of a hot and dense fluid-like medium or QGP is not expected.

Control measurements are however needed to characterize the extent to which initial-state effects can be demarcated from the effects due to the final-state interactions in the QGP.

The p+A collisions due to the absence of a produced medium are expected to isolate the nuclear effects from the initial state of the hard-scattering process. Also the system size evolution at freeze-out can be studied from the small systems (like p+p and p+A), along with the rescattering effects. some of these assumptions are being tested and understood carefully both in Large Hadron Collider (LHC) and in Relativistic Heavy Ion Collider (RHIC) data and more can be possible in future at Electron Ion Collider (EIC).

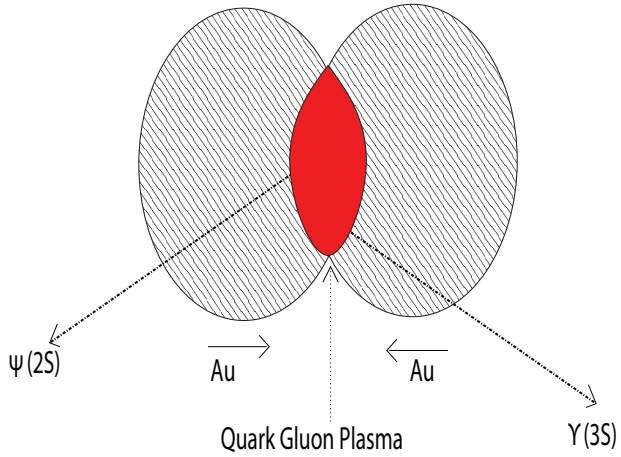

Figure 15: Au-Au collisions producing Ψ(2*S*), and (3*S*), from the QGP.

Citation: Kisslinger LS. Review the Evolution of the Universe. Ann Math Phys. 2025;8(2):073-083. Available from: https://dx.doi.org/10.17352/amp.000149

As was reviewed in the first part of this section and the QGP was inferred through the production of $\Psi(2S)$ and $(3S)$ mesons in Au-Au collisions.

8. The Electroweak Phase Transition (EWPT) and magnetic field creation

Particles get mass, magnetic fields created, Baryogenesis–more quarks than anti-quarks

Fermions (spin 1/2 particles) are (e^-, ν_e) and the μ and τ leptons, and the quarks (q_u, q_d) and the other two quark generations.

Gauge bosons (spin 1 particles) are W^+, W^-, Z^0 and photon (γ). Scalar boson (spin 0) is Higgs, φ_H

At the LHC (Large Hadron Collider) one has found the Higgs mass $\simeq 125\ \text{GeV}$ and CP = Charge-Parity

Production of W^+, W^-, and is shown in the Figure 16 below

With a First Order (EWPT):

1) Critical Temperature, $T_c \simeq 100 - 150\ \text{GeV}$

2) Latent heat = $< \phi_H > \equiv v$

3) Bubbles of the new universe form ($< \phi_H > \equiv v$) inside the old universe ($< \phi_H > \equiv 0$). This gives the Standard Model particles their masses:

$$M_W = gv/\sqrt{2} \quad g = \textit{strong coupling constant}$$
$$M_Z = m_W/\cos(\theta_W) \quad \theta_W = \textit{Weinberg angle} \qquad (24)$$
$$m_e \propto m_u \propto m_d \propto v.$$

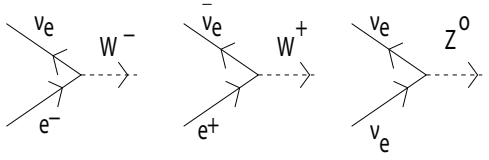

Lepton weak interaction conserves CP–No Baryogenesis

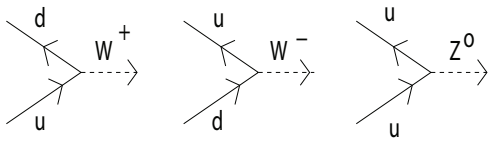

Quark weak interaction violates CP–Baryogenesis Possible

Baryogenesis requires a first order EWPT

Figure 16: Lepton and Quark weak interactions.

Standard Model M_W = 80 GeV and M_Z = 90 GeV.

Bubbles nucleate, creating electromagnetic fields, and collide, creating magnetic fields. These magnetic fields could explain the mystery of gallactic and inter-gallactic magnetic fields, as discussed below.

EW-MSSM Theory. The MSSM (Minimal Supersymmetry Model) another scalar boson field, the Stop (φ_s) is added to the Standard Model Fermion and Boson fields. This has been shown to lead to a first order EWPT.

Electroweak Minimal Supersymmetry Model (EW-MSSM)

All Supersymmetry partners of Standard model particles except the top quark, ϕ_S, are integrated out, giving an EW-MSSM Lagrangian:

$$L^{MSSM} = L^1 + L^2 + L^3$$
$$+ \textit{leptonic and quark interactions}$$
$$L^1 = -\frac{1}{4} W^i_{\mu\nu} W^{i\mu\nu} - \frac{1}{4} B_{\mu\nu} B^{\mu\nu}$$
$$L^2 = |(i\partial_\mu - \frac{g}{2}\tau \cdot W_\mu - \frac{g'}{2} B_\mu)\Phi|^2 - V(\Phi) \qquad (25)$$
$$L^3 = |(i\partial_\mu - \frac{g_s}{2}\lambda^a C^a_\mu)\Phi_s|^2 - V_{hs}(\Phi_s, \Phi),$$

where

$$W^i_{\mu\nu} = \partial_\mu W^i_\nu - \partial_\nu W^i_\mu - g\epsilon_{ijk} W^j_\mu W^k_\nu$$
$$B_{\mu\nu} = \partial_\mu B_\nu - \partial_\nu B_\mu, \qquad (26)$$

where the W^i, with i = (1,2), are the W^+, W^- fields, C^a_μ is an SU(3) gauge field, (Φ, Φ_s) are the (Higgs, right-handed Stop fields), (τ^i, λ^a) are the (SU(2),SU(3) generators, and the electromagnetic and Z fields are defined as

$$A^{em}_\mu = \frac{1}{\sqrt{g^2 + g'^2}} (g' W^3_\mu + g B_\mu)$$
$$Z_\mu = \frac{1}{\sqrt{g^2 + g'^2}} (g W^3_\mu - g' B_\mu). \qquad (27)$$

Electromagnetic field creation during EWPT bubble nucleation (due to spatial symmetry, no magnetic field is created)

B (magnetic) field creation via EWPT bubble collisions (Figure 17)

Results for B (magnetic) field creation via EWPT bubble collisions (Figure 18):

Citation: Kisslinger LS. Review the Evolution of the Universe. Ann Math Phys. 2025;8(2):073-083. Available from: https://dx.doi.org/10.17352/amp.000149

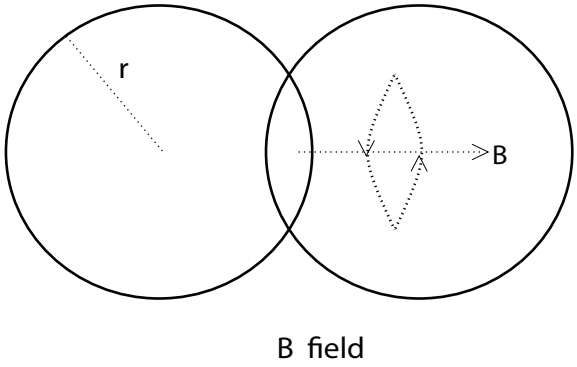

Figure 17: Magnetic field created during EWPT bubble collisions.

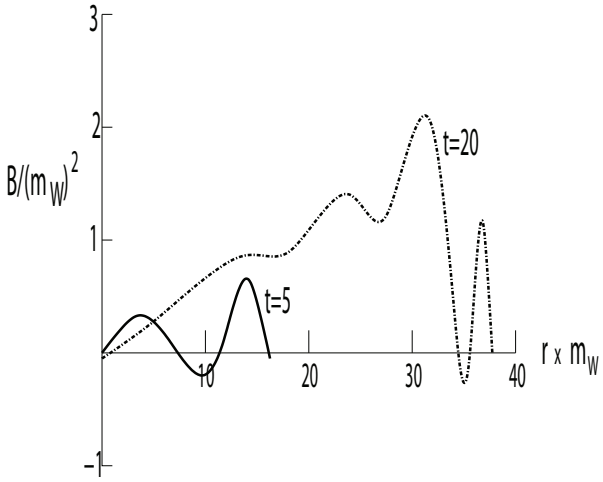

Figure 18: Final Magnetic fields created for two different t as a function of the W mass.

The B-field at the end of the EWPT, with the temperature = T_c, was found to be

$$B^{EWPT}(T_c) = 10M_W^2 \text{ with } M_W = 80 \text{ GeV}$$

$B^{EWPT}(T_c)$ is needed for the estimates of gravitational radiation.

9. Galaxy rotation and dark matter

Our galaxy, the Milky Way, is a gargantuan collection of stars, gas, dust, with a massive black hole held together by gravity. Gravity does not collapse due to the centripetal force.

By measuring the galaxy radius, its speed, and the amount of visible mass, the amount of dark matter mass can be estimated. This is illustrated in the Figure 19 below.

From the measurements illustrated in the Figure above it is estimated that about 24% of the Milky Way galaxy mass is Dark Matter and this includes the mass of the supermassive black hole at the center of the galaxy. This is consistent with the Evolution of the Universe reviewed in section 2.

10. Sterile neutrinos as dark matter

Sterile neutrinos are a well-known source of Dark Matter. For many years the MiniBooNE Collaboration has studied neutrino oscillations. The MiniBooNE Collaboration detected a sterile neutrino ν_4 using $\overline{\nu}_\mu \to \overline{\nu}_e$ oscillations and, estimated the mass difference between this sterile neutrino and a standard neutrino as

$$\Delta m^2 = m_4^2 - m_1^4 \simeq 0.06(eV)^2, \quad (28)$$

which is too small for sterile neutrino ν_4 to be a WIMP (Weakly Interacting Massive Particle).

The notation for the three active neutrinos $\nu_e = \nu_1, \nu_\mu = \nu_2, \nu_\tau = \nu_3$ and the three sterile neutrinos are ν_4, ν_5, ν_6

$$\mathcal{P}(\nu_\mu \to \nu_e) = Re[\sum_{i=1}^{6}\sum_{j=1}^{6} U_{1i}U_{1j}^{*}U_{2i}^{*}U_{2j}e^{-i(\delta m_{ij}^2/E)L}], \quad (29)$$

where neutrinos with flavors ν_e, ν_μ, ν_τ and three sterile neutrinos, $\nu_{s_1}, \nu_{s_2}, \nu_{s_3}$ are related to neutrinos with definite mass by

$$\nu_f = U\nu_m, \quad (30)$$

Where U is a 6x6 matrix. In Ref [9] the sterile-active neutrino mixing angles were calculated, which should be useful for future searches for sterile neutrinos as Dark Matter particles.

Recently the MiniBooNE Collaboration has carried out a search for sub-Gev Dark Matter at the Fermilab [32], with the estimate

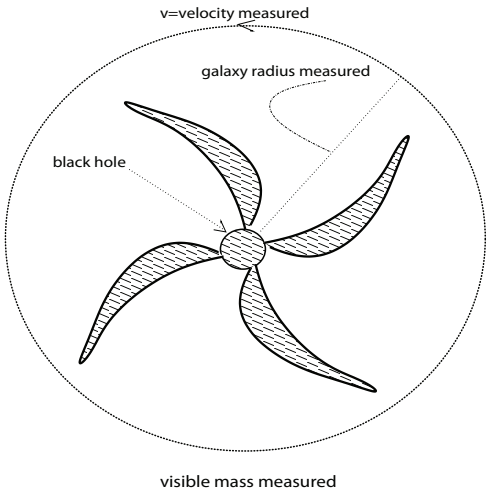

Figure 19: Milky Way galaxy radius, velocity, visible mass measured.

Citation: Kisslinger LS. Review the Evolution of the Universe. Ann Math Phys. 2025;8(2):073-083. Available from: https://dx.doi.org/10.17352/amp.000149

$$200\ \text{MeV} < M_{\nu_{s3}} < 1250\ \text{MeV}. \quad (31)$$

Thus, it is likely that most of the Dark Matter in the Universe consists of sterile neutrinos.

11. Result and Conclusion

The following sections provide a comprehensive review of various topics in physics. Section 2 explores the evolution of the universe, with a focus on quarks and gluons. Section 3, including subsection 3.1, discusses elementary particles, basic forces, and quantum chromodynamics, highlighting the magnitude of the quark-gluon coupling constant. Section 4, along with subsections 4.1 to 4.3, examines differential rapidity cross sections for the production of heavy quark states and their generation in p-p, Xe-Xe, and O-O collisions at 5.44 TeV.

Section 5, with subsection 5.1, analyzes suppression effects, mixed hybrid theory, and suppression phenomena in Xe-Xe collisions, noting that moderate suppression could be measured in future CERN experiments. Section 6 reviews QCDPT, the Quark-Gluon Condensate, and the Quark-Gluon Plasma (QGP), with hybrid meson production via Au-Au collisions potentially signaling QGP formation. Section 7 covers EWPT and magnetic field creation.

Sections 8 and 9 delve into astrophysical phenomena, including galaxy rotation and dark matter, as well as sterile neutrinos as a form of dark matter."

Acknowledgement

Author L.S.K. acknowledges support in part by a grant from the Pittsburgh Foundation.

References

1. Kisslinger LS, Das D. Heavy quark state production in Pb-Pb collisions at $\sqrt{S_{NN}} = 5.02$ TeV . J High Energy Phys. 2017;2017(9):105. Available from: https://doi.org/10.1007/JHEP09%282017%29105

2. Kisslinger LS. Mixed heavy quark hybrid mesons, decay puzzles, and RHIC. Phys Rev D. 2009;79(11):114026. Available from: https://journals.aps.org/prd/abstract/10.1103/PhysRevD.79.114026

3. Kisslinger LS, Das D. Ψ(2S) and Υ(3S) suppression in p-Pb 8 TeV collisions and mixed heavy quark hybrid mesons. Int J Theor Phys. 2016;55(12):5152–8. Available from: https://link.springer.com/article/10.1007/s10773-016-3136-2

4. LHCb collaboration. J High Energy Phys. 2018;2018(11):194.

5. Kisslinger LS, Liu MX, McGaughey P. Heavy-quark-state production in π collisions at GeV. Phys Rev C. 2014;89(2):024914. Available from: https://doi.org/10.1103/PhysRevC.89.024914

6. Cho PL, Leibovich AK. Color-octet quarkonia production. Phys Rev D. 1996;53(1):150–62. Available from: https://doi.org/10.1103/PhysRevD.53.150

7. Braaten E, Chen YQ. Helicity decomposition for inclusive $\frac{J}{\psi}$ production. Phys Rev D. 1996;54(5):3216–22. Available from: https://doi.org/10.1103/PhysRevD.54.3216

8. Braaten E, Fleming S. Color-octet fragmentation and the ' surplus at the Fermilab Tevatron. Phys Rev Lett. 1995;74(17):3327–30. Available from: https://doi.org/10.1103/PhysRevLett.74.3327

9. Kisslinger LS. Neutrino oscillations with three active and three sterile neutrinos. Int J Theor Phys. 2016;55(10):3274–81. Available from: https://link.springer.com/article/10.1007/s10773-016-2957-3

10. Kisslinger LS, Das D. Review of QCD, quark–gluon plasma, heavy quark hybrids, and heavy quark state production in p-p and A-A collisions. Int J Mod Phys A. 2016;31(13):1630010. Available from: https://doi.org/10.1142/S0217751X16300106

11. ALICE Collaboration. Inclusive J/ψ production in Xe–Xe collisions at $\sqrt{S_{NN}} = 5.44$ TeV = 5.44 TeV. Phys Lett B. 2018;785:419–28. Available from: https://doi.org/10.1016/j.physletb.2018.08.047

12. Particle Data Group. Particle Physics Booklet. 2020.

13. CTEQ Collaboration. CTEQ6 Parton Distributions. Available from: http://hep.pa.msu.edu/cteq/public/cteq6.html

14. Kisslinger LS, Liu MX, McGaughey P. Heavy-quark-state production in p–p collisions. Phys Rev D. 2011;84(11):114020. Available from: https://doi.org/10.1103/PhysRevD.84.114020

15. Shifman MA, Vainstein AI, Zakharov VI. QCD and resonance physics. Applications. Nucl Phys B. 1979;147:385–447. Available from: https://doi.org/10.1016/0550-3213(79)90023-3

16. 16. Abelev BI, Aggarwal MM, Ahammed Z, Anderson BD, Arkhipkin D, Averichev GS, et al. J/ψ production at high transverse momenta in p+p and Cu+Cu collisions at $\sqrt{S_{NN}} = 200$ GeV . Phys Rev C. 2009;80(4):041902. Available from: https://doi.org/10.1103/PhysRevC.80.041902

17. 17. Adler C, Ahammed Z, Allgower C, Amonett J, Anderson BD, Anderson M, et al. Centrality dependence of high-pT hadron suppression in Au+Au collisions at $\sqrt{S_{NN}} = 130$ GeV . Phys Rev Lett. 2002;89(20):202301. Available from: https://doi.org/10.1103/PhysRevLett.89.202301

18. Adare A, Afanasiev S, Aidala C, Ajitanand NN, Akiba Y, Al-Bataineh H, et al. J/ψ production in Cu+Cu collisions. Phys Rev Lett. 2008;101(12):122301. Available from: https://doi.org/10.1103/PhysRevLett.101.122301

19. Adare A, Afanasiev S, Aidala C, Ajitanand NN, Akiba Y, Al-Bataineh H, et al. Energy loss and flow of heavy quarks in Au+Au collisions at $\sqrt{S_{NN}} = 200$ GeV . Phys Rev Lett. 2007 Apr;98(17):172301. Available from: https://doi.org/10.1103/PhysRevLett.98.172301

20. Adare A, Afanasiev S, Aidala C, Ajitanand NN, Akiba Y, Al-Bataineh H, et al. Energy loss and flow of heavy quarks in Au+Au collisions at $\sqrt{S_{NN}} = 200$ GeV . Phys Rev Lett. 2007;98(19):192301. Available from: https://doi.org/10.1103/PhysRevLett.98.172301

21. Karsch F, Kharzeev D, Satz H. Sequential charmonium dissociation. Phys Lett B. 2006;637(1-2):75–80. Available from: https://doi.org/10.1016/j.physletb.2006.03.078

22. Vitev I, Goldman T, Johnson MB, Qiu JW. Open charm tomography of cold nuclear matter. Phys Rev D. 2006;74(5):054010. Available from: https://doi.org/10.1103/PhysRevD.74.054010

23. Sharma R, Vitev I, Zhang BW. Light-cone wave function approach to open

Citation: Kisslinger LS. Review the Evolution of the Universe. Ann Math Phys. 2025;8(2):073-083. Available from: https://dx.doi.org/10.17352/amp.000149

heavy flavor dynamics in QCD matter. Phys Rev C. 2009;80(5):054902. Available from: https://doi.org/10.1103/PhysRevC.80.054902

24. Adler C, Ahammed Z, Allgower C, Amonett J, Anderson BD, Anderson M, et al. Multiplicity distribution and spectra of negatively charged hadrons in Au+Au collisions at $\sqrt{S_{NN}} = 130$ GeV. Phys Rev Lett. 2001;87(11):112303. Available from: https://doi.org/10.1103/PhysRevLett.87.112303

25. Baumgart S (STAR Collaboration). High-pT Hadron Suppression in Au+Au Collisions at RHIC. arXiv preprint arXiv:0709.4223 [nucl-ex]. 2007. Available from: https://arxiv.org/abs/0709.4223

26. Loizides C, Kamin J, d'Enterria D. Improved Monte Carlo Glauber predictions at present and future nuclear colliders. Phys Rev C. 2019;97(5):054910. Available from: https://doi.org/10.1103/PhysRevC.97.054910. Available from: https://arxiv.org/abs/1710.07098 [nucl-ex]

27. Qiu JW, Vitev I. Resummed QCD power corrections to nuclear shadowing. Phys Rev Lett. 2004;93(26):262301. Available from: https://doi.org/10.1103/PhysRevLett.93.262301

28. Brewer J, Mazeliauskas A, van der Schee W. Opportunities of OO and pO collisions at the LHC. arXiv preprint arXiv:2103.01939. Available from: https://arxiv.org/abs/2103.01939

29. Kharzeev D, Satz H. Charmonium composition and nuclear suppression. Phys Lett B. 1996;366(4):316–322. Available from: https://doi.org/10.1016/0370-2693(95)01328-8

30. Adare A, Aidala C, Ajitanand NN, Akiba Y, Al-Bataineh H, Alexander J, et al. Nuclear modification of Ψ', xc and J/ψ production in d+Au collisions at $\sqrt{S_{NN}} = 200$ GeV. Phys Rev Lett. 2013;111(20):202301. Available from: https://doi.org/10.1103/PhysRevLett.111.202301

31. Abelev B, Adam J, Adamová D, Aggarwal MM, Agnello M, Agostinelli A. Suppression of ψ(2S) production in p-Pb collisions at $\sqrt{S_{NN}} = 5.02$ TeV. J High Energy Phys. 2014;2014(12):073. Available from: https://link.springer.com/article/10.1007/JHEP12(2014)073

32. Aguilar-Arevalo AA, Brown BC, Conrad JM, Dharmapalan R, Diaz A, Djurcic Z. Updated MiniBooNE neutrino oscillation results with increased data and new background studies. Phys Rev D. 2021;103(5):052002. Available from: https://doi.org/10.1103/PhysRevD.103.052002

33. Abe F, Akimoto H, Akopian A, Albrow MG, Amendolia SR, Amidei D, et al. Production of J/ψ mesons from χc meson decays in $p\overline{p}$ collisions at the $\sqrt{S} = 1.8$ TeV. Phys Rev Lett. 1997 Jan;79(5):578. Available from: https://doi.org/10.1103/PhysRevLett.79.578

34. Vogel H. Proceedings of the 4th Flavor Physics and CP Violation Conference (FPCP'06). 2006. Available from: https://inspirehep.net/conferences/977181

35. Kisslinger LS. Ψ(2S), Υ(3S) suppression in p-Pb, Pb-Pb collisions and mixed hybrid theory. Int J Theor Phys. 2016 Aug;54(5):1847–1853. Available from: https://link.springer.com/article/10.1007/s10773-015-2824-7

Citation: Kisslinger LS. Review the Evolution of the Universe. Ann Math Phys. 2025;8(2):073-083. Available from: https://dx.doi.org/10.17352/amp.000149